Environmental Science & Technology

pubs.acs.org/est

Article

Microaerophilic Oxidation of Fe(II) Coupled with Simultaneous Carbon Fixation and As(III) Oxidation and Sequestration in Karstic Paddy Soil

Hui Tong, Chunju Zheng, Bing Li, Elizabeth D. Swanner, Chengshuai Liu,* Manjia Chen, Yafei Xia, Yuhui Liu, Zengping Ning, Fangbai Li, and Xinbin Feng

Cite This: *Environ. Sci. Technol.* 2021, 55, 3634−3644

Read Online

ACCESS | Metrics & More | Article Recommendations | Supporting Information

ABSTRACT: Microaerophilic Fe(II)-oxidizing bacteria are often chemolithoautotrophs, and the Fe(III) (oxyhydr)oxides they form could immobilize arsenic (As). If such microbes are active in karstic paddy soils, their activity would help increase soil organic carbon and mitigate As contamination. We therefore used gel-stabilized gradient systems to cultivate microaerophilic Fe(II)-oxidizing bacteria from karstic paddy soil to investigate their capacity for Fe(II) oxidation, carbon fixation, and As sequestration. Stable isotope probing demonstrated the assimilation of inorganic carbon at a maximum rate of 8.02 mmol C m^{-2} d^{-1}. Sequencing revealed that *Bradyrhizobium*, *Cupriavidus*, *Hyphomicrobium*, *Kaistobacter*, *Mesorhizobium*, *Rhizobium*, unclassified *Phycisphaerales*, and unclassified *Opitutaceas* were fixing carbon. Fe(II) oxidation produced Fe(III) (oxyhydr)oxides, which can absorb and/or coprecipitate As. Adding As(III) decreased the diversity of functional bacteria involved in carbon fixation, the relative abundance of predicted carbon fixation genes, and the amount of carbon fixed. Although the rate of Fe(II) oxidation was also lower in the presence of As(III), over 90% of the As(III) was sequestered after oxidation. The potential for microbially mediated As(III) oxidation was revealed by the presence of arsenite oxidase gene (*aioA*), denoting the potential of the Fe(II)-oxidizing and autotrophic microbial community to also oxidize As(III). Thisstudy demonstrates that carbon fixation coupled to Fe(II) oxidation can increase the carbon content in soils by microaerophilic Fe(II)-oxidizing bacteria, as well as accelerate As(III) oxidation and sequester it in association with Fe(III) (oxyhydr)oxides.

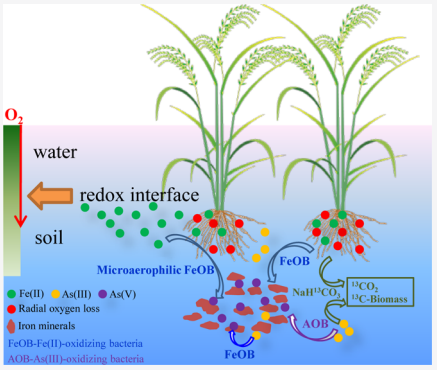

KEYWORDS: *microaerophilic Fe(II)-oxidizing bacteria, karstic soils, carbon fixation, As oxidation, As sequestration*

INTRODUCTION

Karst constitutes 33% of the total land area of China, approximately 3.44 × 10^6 km^2,[1] and the karst region in southwest China is one of the largest continuous karst areas on the Earth. The ecosystems of this region are vulnerable to disturbances and are experiencing land degradation such as soil erosion and rocky desertification. In this area, a large amount of paddy soil suffers from karst rocky desertification, characterized by an increase in the abundance of inorganic carbon and a reduction in land productivity.[2] Besides karst rocky desertification, paddy soil in this area contains 2.5 million tons of explored arsenic (As) resources, accounting for 60% of the total explored As in China,[3] and is heavily polluted by As because of mining and smelting. Wastewater containing As derived from industrial activities, including mine tailings and industrial waste residues, contaminates soil through various channels.[4] In the porous karst region, surface water and rainfall are quickly transported through soil, making soil and groundwater vulnerable to As pollution.[3] These problems seriously hinder the sustainability of soil and water resources in this region. However, the presence of inorganic carbon might facilitate the growth of chemolithoautotrophs that accelerate the transformation of inorganic carbon to organic carbon.[5] This process could sustain the resilience of the ecosystem and increase the soil fertility. Therefore, solutions are needed to improve the transformation of inorganic carbon to bioavailable organic carbon and minimize the effect of As contamination.

Because of the specific geochemistry of karst rocky desertification, carbonate increases from limestone dissolution. Recent reports have shown that the elevated carbonate could facilitate the enrichment of chemolithoautotrophs in karstic soils.[5,6] Chemolithoautotrophs are a functional class of microorganisms that can conserve energy through the oxidation of

Received: August 28, 2020
Revised: December 28, 2020
Accepted: December 29, 2020
Published: January 7, 2021

https://dx.doi.org/10.1021/acs.est.0c05791
Environ. Sci. Technol. 2021, 55, 3634−3644

inorganic electron donors such as iron, sulfide, sulfur, metals, nitrite, hydrogen gas, and carbon monoxide.[7] These microorganisms play a crucial role in inorganic carbon fixation in the global carbon cycle.[8,9] For example, chemolithoautotrophs from the Yellowstone National Park incorporated a minimum of 42% dissolved inorganic carbon into biomass carbon under Fe(II) oxidation conditions,[10] demonstrating that in some environments, chemolithoautotrophs can dominate carbon fixation processes.

The paddy soils in southwest China are red soils that contain abundant iron. The reduced form of Fe is an inorganic electron donor that can fuel chemolithoautotrophic fixation of inorganic carbon to organic carbon, if a suitable electron acceptor, such as molecular oxygen (O_2), is present. Chemolithoautotrophic Fe(II)-oxidizing bacteria have been isolated from diverse freshwater and marine habitats with gradient tube methods that utilize opposing diffusion gradients of Fe(II) and O_2 to mimic redox boundaries that occur in nature.[11−13] Because of the limited energy released from Fe(II) oxidation with oxygen at circumneutral pH and the fast chemical kinetics of the abiotic reaction at oxygen saturation, most neutrophilic Fe(II)-oxidizing bacteria compete with rapid abiotic processes as microaerophiles.[12] In natural environments, these microorganisms have been shown to actively contribute to net Fe(II) oxidation by up to 89%.[14] This was similar with the maximum biological Fe(II) oxidation of 88% in laboratory-controlled setups under micro-oxic conditions (9−50 μM O_2).[12] These reports confirmed the activity and importance of microbial Fe(II) oxidation under micro-oxic conditions. In karstic soils, the thin soil layer and the high hydraulic conductivity within this region could promote the formation micro-oxic conditions. Such micro-oxic Fe(II) oxidation coupled to carbon assimilation are vital geochemical processes for element cycling at oxic−anoxic interface.[15,16] Nevertheless, the diversity and activity of the chemolithoautotrophic Fe(II)-oxidizing bacteria and their ability of carbon fixation in inorganic carbon-enriched karstic soils remain largely unknown.

Microbial pathways responsible for carbon fixation mainly include the Calvin−Benson−Bassham (CBB) cycle, the reductive tricarboxylic acid cycle, reductive acetyl-CoA pathway, 3-hydroxypropionate/4-hydroxybutyrate cycle, and the dicarboxylate/4-hydroxybutyrate cycle.[9] According to metagenomic analysis, the CBB cycle is considered to be the most significant carbon fixation pathway by microaerophilic Fe(II)-oxidizing bacteria in circumneutral conditions.[15,17] Geochemical approaches such as stable isotope probing (SIP) with $^{13}CO_2$ can quantify CO_2 fixation in samples or incubations containing chemolithoautotrophic Fe(II)-oxidizing bacteria. Furthermore, SIP with $^{13}CO_2$ can also be leveraged to identify microorganisms responsible for the fixation of CO_2 in microbial communities, as their DNA becomes ^{13}C-labeled. This DNA can subsequently be identified by various molecular techniques, such as DNA fingerprinting and high-throughput sequencing.[18,19]

The iron minerals formed by Fe(II)-oxidizing bacteria have been identified as the key sorbents that sequester heavy metals in natural environments.[20−22] Generally, at circumneutral pH, the resulting minerals are poorly crystalline Fe(III) (oxyhydr)oxides with a high specific surface area, positive surface charges, and abundant adsorption sites, which make a significant impact on contaminant removal, including phosphorus and As.[22−24] Fe(III) (oxyhydr)oxides adsorb both As(III) and As(V) at circumneutral pH.[25] e(III) (oxyhydr)oxides have a higher adsorption capacity for As(V) than As(III) when the pH is below 7.[26] Therefore, oxidation of As(III) to As(V) could potentially enhance the sequestration of As on Fe(III) (oxyhydr)oxides at circumneutral pH. A previous report has demonstrated that several autotrophic Fe(II)-oxidizing bacteria can also oxidize As(III).[27] These Fe(II)-oxidizing bacteria might oxidize Fe(II) and As(III) simultaneously while fixing inorganic carbon. These co-occurring processes could increase the soil fertility by converting inorganic to organic carbon and reduce As pollution in areas affected by karst rocky desertification. However, other than As immobilization with Fe(II)-oxidizing bacteria in pure cultures, the detection and quantification of chemolithoautotrophic bacteria with the capacity of Fe(II) oxidation and carbon fixation and their function in As oxidation following sequestration in karst rocky desertification areas have yet to be investigated in detail.

Considering the research gaps mentioned above, the combination of gradient tube enrichments, stable ^{13}C probing, and high-throughput sequencing were used to identify paddy soil microorganisms involved in carbon fixation, Fe(II) oxidation, and As sequestration in karstic soils from southwest China. The primary objectives of this study were to (i) evaluate the extent of microbial CO_2 fixation by chemoautotrophic communities during micro-oxic Fe(II) oxidation, (ii) identity the related microorganisms responsible for carbon fixation coupled with Fe(II) oxidation, and (iii) elucidate the mechanism of As sequestration in the presence of these processes.

MATERIALS AND METHODS

Chemicals. As(III) and As(V) stock solutions (20 mM) were prepared by dissolving sodium As ($NaAsO_2$) and disodium hydrogen arsenate heptahydrate salt ($AsHNa_2O_4{\cdot}7H_2O$), respectively, followed by nylon filter sterilization (0.22 μm, Fisher Scientific). The [^{13}C]-$NaHCO_3$ (99% atom ^{13}C) was obtained from Cambridge Isotope Laboratories (Cambridge, MA, USA). All the other analytical grade chemicals were obtained from the Guangzhou Chemical Co. (Guangzhou, China). All solutions were prepared using deionized water (18.2 MΩ) from an ultrapure water system (Easy Pure II RF/UV, Thermo Scientific, USA).

Site Description and Sampling. A paddy soil sample containing orange/brick red-colored flocs was collected from Xingren County, Southwest China (25°32′31.2″N, 105°30′25.2″E). The physicochemical properties of the paddy soil are shown in Table S1. During sample collection, four equally sized subsamples were collected from the surface (25 cm length × 25 cm width × 10−20 cm depth) and they were mixed to form a bulk soil sample. This composite sample was then quartered to obtain the soil samples for laboratory incubation and analysis. Based on the oxygen concentration with depth (data not shown), the 10−20 cm depth of soil as a micro-oxic zone was collected to incubate microaerophilic Fe(II)-oxidizing bacteria. The sample used for cultivation was immediately transferred into polyvinyl chloride bottles upon collection and then stored at 4°C in a portable cooler. The soil sample for DNA analysis was frozen and stored in dry ice and then transferred for storage at −80°C in a laboratory.

Cultivation of Soil Microbes. A gradient tube approach was utilized to cultivate Fe(II)-oxidizing bacteria,[11] in which opposing O_2 and Fe(II) gradients developed within a semisolid agar overlaying an agar-stabilized mineral Fe(II) source. This produces an interface of anoxic and Fe(II)-bearing media with micro-oxic conditions that allows for the growth of micro-

https://dx.doi.org/10.1021/acs.est.0c05791
Environ. Sci. Technol. 2021, 55, 3634−3644

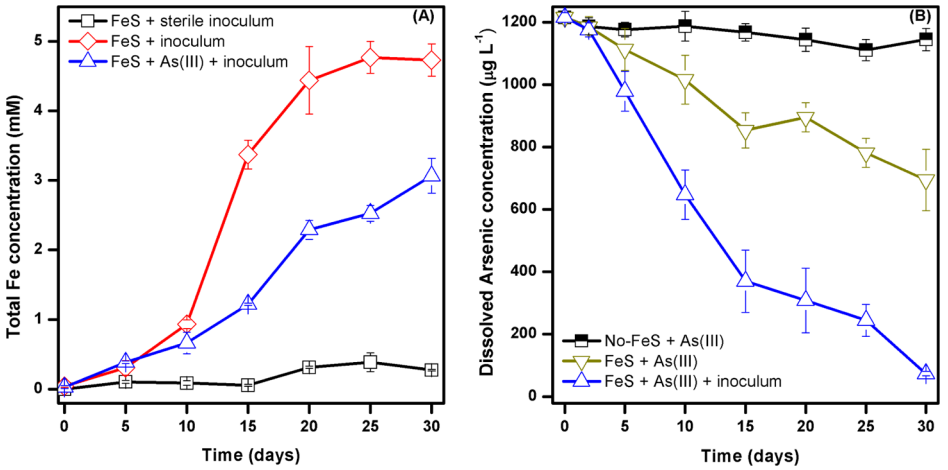

Figure 1. (A) Concentration of total Fe in the growth bands for all treatments and (B) dissolved As [As(III) + As(V)] concentrations in the dissolved phase from the growth bands during the incubation. For all treatments, including the inoculated and control treatments, the samples for total Fe and As were collected at the same depth intervals of the gradient tubes. Error bars show the standard deviation of the three replicates.

aerophilic Fe(II)-oxidizing bacteria. Iron sulfide (FeS) was used as an Fe(II) source.[11] All gradient media consisted of bicarbonate-buffered Modified Wolfe's Mineral Medium (MWMM), which was bubbled with filter-sterilized CO_2. The MWMM (1 L) was composed of 1 g of NH_4Cl, 0.2 g of $MgSO_4 \cdot 7H_2O$, 0.1 g of $CaCl_2 \cdot 2H_2O$, and 0.05 g of K_2HPO_4.[11] Screw-capped 20 × 125 mm (25 mL) disposable tubes were used as vessels for gradient tube cultures. The bottom layer consisted of 3 mL FeS per tube, with equal volumes of the FeS suspension and MWMM medium, stabilized with 1% (w/v) agarose. The top layer was 14 mL of MWMM medium with 5 mM sodium bicarbonate and 1 μL of vitamins solution and trace minerals per milliliter of medium, made semisolid by adding 0.15% (w/v) agarose. The pH of semisolid gradient medium was adjusted to 6.2 by bubbling with sterile CO_2 gas. To inoculate the gradient tubes, equal quantities of soil and sterile soil were mixed and a 10 μL of suspension was drawn into a pipette tip and inserted through the agar overlay. After 20 days of incubation, 20 μL of the incubated microcosm was transferred to a new gradient tube. Serial transfers were performed for four generations before being transferred to fresh gradient tubes that were used for As immobilization and carbon fixation experiments. These enriched microorganisms are henceforth referred to as the "original inoculum". For As immobilization experiments, 16 μM of As(III) from sterile 20 mM $NaAsO_2$ stock solutions was added to semisolid gradient medium based on the As concentration in southwest China in previous reports.[3,28] For carbon fixation experiments, $NaHCO_3$ was prepared as $^{12}C-NaHO_3$ and $^{13}C-NaHO_3$, while all other conditions were same as the As immobilization experiments. Enrichment experiments were performed at a constant temperature of 25 ± 1 °C in a dark incubator. At specific intervals (t = 0, 5, 10, 15, 20, 25, and 30 days), the gradient tubes were taken out to measure total Fe and dissolved As concentrations and to perform DNA extraction.

Iron, As, Sulfur Species, and Excreted Organic Acid Determination. Total iron concentrations in the growth band which formed within the overlay were measured using Ferrozine following treatment with the reducing reagent hydroxylamine hydrochloride.[11] Methods for sample collection and analysis are described in Supporting Information (Text S1). In the inoculated experiments, the entire growth band was collected and filtered to determine the As concentration [as total As, As(III), and As(V)]. In the sterile control and no-FeS experiments, the semisolid medium from the same depth in the gradient tubes as total Fe was measured and collected to determine the total As concentration in the aqueous phase (dissolved), immobilized on the surface co-precipitated with Fe(III) (oxyhydr)oxides. Methods for separating the dissolved As, absorbed As, co-precipitated As, and methylated As determination are described in Supporting Information (Text S2). The details of sulfur species determination are described in Text S3, Supporting Information. The excreted organic acids during incubation were determined by high-pressure liquid chromatography and ion chromatography, following the method in previous reports (Text S3, Supporting Information).

Mineral Characterization, Confocal Laser Scanning Microscopy, and Microbial Biomass C. The detailed procedures used for Mössbauer spectroscopy, X-ray diffraction (XRD), confocal laser scanning microscopy (CLSM), chloroform fumigation extraction, and total organic carbon analyzer are provided in Text S4, Supporting Information.

DNA Extraction, Real-Time PCR, Isopycnic Centrifugation, High-Throughput Amplicon Sequencing, and Bioinformatics Analysis. Approximately 0.3 g iron minerals (contained the growth band and agarose around the growth band) were collected by centrifugation in ^{13}C-labeled or unlabeled $NaHCO_3$ experiments. The DNA from three replicates of experiments at each sampling time was extracted using a PowerSoil DNA isolation kit (MO BIO Laboratories, Inc., Carlsbad, CA, USA). The DNA was quantified by a Qubit 2.0 Fluorometer (Invitrogen, Carlsbad, CA, USA), and the procedures for DNA separation by isopycnic centrifugation are described in Supporting Information (Text S5). Polymerase chain reaction (PCR) amplification of 16S rRNA gene fragments (V4 region) was carried out with Illumina-specific fusion bacterial primers, that is, F515 and R806 with a sample-specific 12-bp barcode added to the reverse primer for both total genomic DNA extracts and DNA fractions separated by isopycnic centrifugation.[29] The details for PCR amplification, real-time PCR, Illumina sequencing, and bioinformatics analysis are given in Supporting Information (Text S5). The sequence data sets are deposited in the NCBI under BioProject ID PRJNA381404 and accession number SRP063292.

https://dx.doi.org/10.1021/acs.est.0c05791
Environ. Sci. Technol. 2021, 55, 3634−3644

RESULTS

Fe(III) (Oxyhydr)oxide Formation and As Sequestration during Microaerophilic Microbial Fe(II) Oxidation. Five days after inoculation of the environmental samples into gradient tubes, a zone of Fe(II) oxidation was visible because of the appearance of thin orange Fe(III) (oxyhydr)oxides at an intermediate distance between the FeS plug in the bottom of the tube and the air interface at the surface of the gel (Figure S1). In the sterile treatments, abiotic Fe(II) oxidation occurred lower in the tube than in the inoculated treatments and was dispersed throughout most of the medium. The oxygen concentration at the top of the thin Fe(III) layer was around 60 μM, and no oxygen was detected at the bottom of thin Fe(III) (oxyhydr)-oxides (data not shown). The low oxygen conditions comprise a micro-oxic region for microaerophilic bacteria growth. The total Fe concentration in Fe(III) (oxyhydr)oxides layer is shown in Figure 1A (original data shown in Table S3). The rate of Fe(II) oxidation, calculated from a pseudo first-order exponential decay model with the data in Figure 1A, was higher in treatments without As(III) (0.153 mM d^{-1}) than that with As(III) (0.114 mM d^{-1}). When the reversible dissociation of FeS yielded Fe(II) in the gradient tubes, it also released some S^{2-}. Compared to the sterile treatment, the results suggested that some $S^{2-}$was oxidized to $SO_4^{2-}$by bacteria (Figure S2). Around the growth bands, a very small amount of HS^- was detected (data not shown). By estimating the sulfur mass balance, some sulfur might volatilize in the form of H_2S.[12]

After the precipitation of iron, the dissolved As concentration decreased (Figure 1). The amount of As removal via sorption and/or coprecipitation is shown in Figure 1B. Concomitantly, the amount of Fe(III) (oxyhydr)oxides increased and the As adsorption on and/or coprecipitation with Fe(III) (oxyhydr)-oxides accelerated. The result shows that 93.4% As removal was obtained by 30 days within the inoculated samples. In the abiotic control (FeS + As(III) treatment), abiotic Fe(II) oxidation by limited oxygen diffusion could also form Fe(III) (oxyhydr)-oxides, which could adsorb and/or co-precipitate As, leading to the decrease of dissolved As concentration. No methylated As was detected in the gradient tubes. Over 80% of the As ultimately was found as As(V) in the inoculated treatments, while only a small amount of As(III) oxidation occurred in the abiotic treatments after incubation for 30 days (Figure S3A), indicating that the enriched Fe(II)-oxidizing bacteria may be responsible for the microbial oxidation of As(III) under micro-oxic conditions. In the inoculated treatment with As(III), the total Fe concentration (~3.1 mM) from Fe(II) oxidation is much higher than As(V) concentration (~12.8 μM) from As(III) oxidation, indicating that the competition for electron acceptors between As(III) and Fe(II) oxidation could be negligible. Therefore, the decrease of total Fe concentration in treatments with As(III) likely resulted from the toxicity of As(III) and/or As(V).

The mineralogy of the precipitates formed in the inoculated gradient tubes was analyzed by XRD and Mössbauer spectroscopy. The results of Mössbauer spectroscopy were obtained at 12K (Figure S4), and the fitting parameters are provided in Table S4. According to the negative quadruple splitting values, the precipitates were identified as ferrihydrite.[30] The Mössbauer data clearly showed that the dominant precipitate phase (>95% of total Fe) was ferrihydrite regardless of the presence or absence of As. A small amount of Fe(II) (<3% of total Fe) was detected in the mineral. In the treatment with As, the precipitates formed both As adsorption and coprecipitation processes as the spectral parameters of sextet Fh3 (CS ≈ 0.35 mm/s and Bhf≈ 50 T) of the precipitates approached values reported for amorphous ferric arsenate.[23] This result was consistent with the XRD pattern that a weak peak appeared around 58° in the presence of arsenic (characterized as poor crystalline ferric arsenate) (Figure S5).

Because As sequestration processes include adsorption and coprecipitation, we used wet chemical extraction with NaOH solution to distinguish between the adsorbed arsenic and coprecipitated arsenic.[31,32] Following NaOH extraction, complete dissolution of the Fe(III) (oxyhydr)oxides led to the recovery of 25 ± 3% of the adsorbed and 73 ± 6% of the coprecipitated As after incubation for 30 days (Figure S6). The results of As speciation showed that most co-precipitated As ultimately existed as As(V) after 30 days of incubation (Figure S3), indicating that As(V) preferentially co-precipitated with the Fe(III) (oxyhydr)oxides during microaerophilic microbial Fe(II) oxidation under micro-oxic conditions. The overall As recovery in these experiments was about 99%.

Bacterial Community Composition with Incubations. High-throughput sequencing was carried out in triplicate on the original inoculum and incubations with or without As(III) at 10, 20, and 30 days. In total, 1,533,834 qualified sequences for the 21 samples analyzed were generated by Illumina high-throughput sequencing after filtering out a poor quality sequence, ranging from an average of 67,822 to 78,942 sequences per sample. The normalization of the clean sequences was conducted by randomly extracting 65,530 clean sequences from each sample data set to fairly compare all samples at the same sequencing depth (Table S5). The α-diversity indexes are listed in Table S5. The high coverage index values indicated that the sequence data were sufficient to effectively characterize bacterial communities. The α-diversity was greater in the absence of As(III). According to the principal coordinates analysis (PCoA) and Chao1 and Simpson indexes, the bacterial communities are significantly different between the treatments with and without As(III) after incubation for 30 days (P< 0.05, Figure S7 and Table S5).

After four transfers of the original inoculum, the dominant genera for inoculation were *Cupriavidus*, *Kaistobacter*, *Mesorhizobium*, *Rhizobium*, *Pseudomonas*, *Polaromonas*, and *Bradyrhizobium*. *Cupriavidus* (33.2%) and *Kaistobacter* (30.5%) were the most abundant genera (Figure 2). After incubation for 30 days, *Rhizobium* increased rapidly and became one of the most abundant genera in treatments with or without As(III), although the relative abundance of *Rhizobium* was higher in the absence of As(III) than that in the presence of As(III). The bacterial community in treatments with As(III) was dominated by *Cupriavidus*, *Rhizobium*, *Bradyrhizobium*, *Kaistobacter*, *Polaromonas*, and *Pseudomonas*.

^{13}C Content of Biomass and Identification of CO_2-Fixing Microorganisms under Fe(II)-Oxidizing Conditions. $NaHCO_3$ was added as inorganic carbon source during the enrichment process. Autotrophic microorganisms assimilated metabolized $^{13}C-NaHCO_3$ to produce ^{13}C-labeled biomass. The assimilation results of ^{13}C $NaHCO_3$ in the biomass are shown in Figure 3. Compared with the control treatment, the yield of ^{13}C biomass increased gradually from 0 to 30 days within the inoculated samples. In addition, there was more ^{13}C-bearing biomass produced in the absence of As than in the presence of As after incubation for 30 days. The maximum carbon assimilation amounts without As(III) and with As(III)

https://dx.doi.org/10.1021/acs.est.0c05791
Environ. Sci. Technol. 2021, 55, 3634−3644

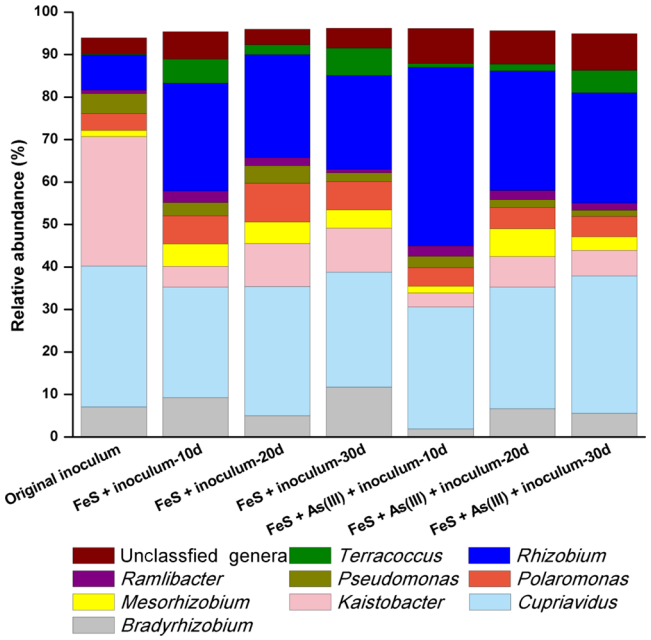

Figure 2. Relative abundance of bacterial genera with a minimum relative abundance greater than 1% in the absence and presence of As(III). The 10d, 20d, and 30d represent incubation for 10, 20, and 30 days, respectively. The relative abundance is presented as the average percentage of the three replicates.

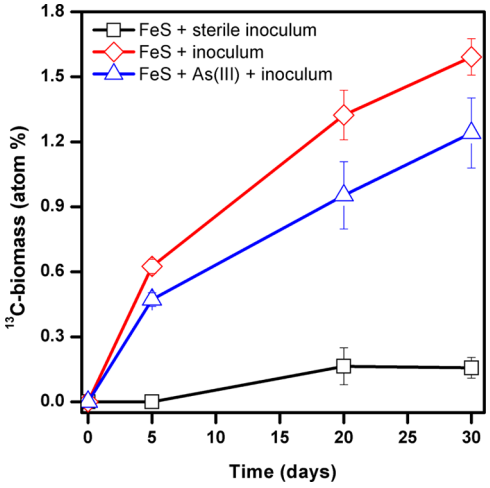

Figure 3. Formation of ^{13}C-biomass from the different treatments with ^{13}C−NaHCO$_3$. Error bars show the standard deviation of the three replicates.

after 30 days of incubation reached 1.6 and 1.2% ^{13}C−NaHCO$_3$, respectively. In order to determine the bacterial genera responsible for autotrophic carbon assimilation in the gradient tubes without As(III) and with As(III), total DNA samples from the labeled and unlabeled ^{13}C−NaHCO$_3$ microcosms were subjected to ultra-centrifugation and fractionation, and each gradient fraction was submitted for high-throughput sequencing. In addition, each gradient fraction was used for quantitative PCR (qPCR) to access comparative DNA distribution in light and heavy fractions (Figure S8). The results showed that the maximum copies had a shift in the heavy fractions between ^{12}C− and ^{13}C−NaHCO$_3$ samples, which indicated that some special bacteria had assimilated ^{13}C and incorporated into their DNA. The peak shift suggested that a portion of ^{13}C (1.2−1.6%) was assimilated by microorganisms within the gradient tubes (Figures 3 and S8).

To analyze the carbon-fixing microorganisms, each DNA gradient fraction in treatments with or without As(III) was subjected to high-throughput 16S rRNA gene sequencing. Based on the differences in the relative abundances in different fractions, eight typical genera were observed in ^{13}C-heavy fractions (Figures 4, S9 and S10). *Cupriavidus* and *Kaistobacter*

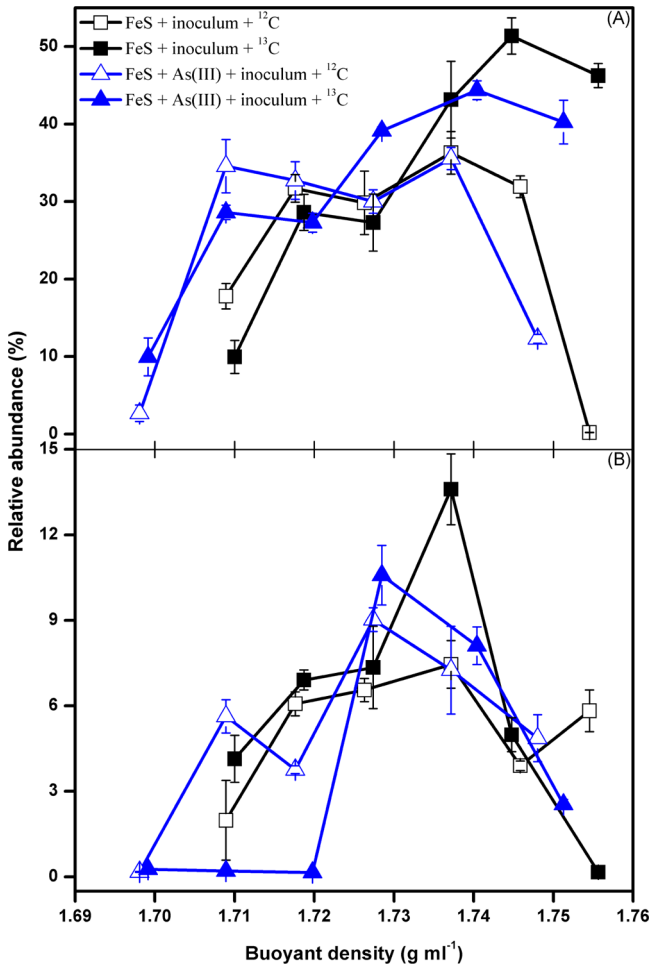

Figure 4. Two most abundant genera (A) *Cupriavidus* and (B) *Kaistobacter* in the heavy fractions from the ^{13}C−NaHCO$_3$ microcosms compared with their abundance in fractions of similar buoyant density from unlabeled NaHCO$_3$ microcosms after 30 days. Error bars show the standard deviation of the three replicates.

enriched in ^{13}C-heavy fractions were observed in both treatments with As(III) or without As(III), whereas their enrichment was not detected in the ^{12}C-heavy fractions (Figure 4). The relative abundances of these two genera in incubations without As(III) were higher than that with As(III). Meanwhile, four microorganisms including *Bradyrhizobium*, *Mesorhizoboium*, *Hyphomicrobium*, and *Rhizobium* were also enriched in incubations without As(III), while unclassified *Phycisphaerales* and unclassified *Opitutaceae* were enriched in ^{13}C-heavy fractions with As(III) (Figures S9 and S10). *Cupriavidus* was the most abundant genus in all treatments and had the highest relative abundances of 51.4 and 44.4% in the absence and presence of As(III), respectively, at a heavy buoyant density of 1.744 mg L^{-1}.

https://dx.doi.org/10.1021/acs.est.0c05791
Environ. Sci. Technol. 2021, 55, 3634−3644

Prediction of Functional Genes Involved in Carbon Fixation and Fe(II) and As(III) Oxidation in Bacterial Community. Twelve genes from the KEGG database were predicted to be involved in iron, carbon, and As metabolism (Figure S11). Several indicator genes of Fe(II) oxidation were predicted by PICRUSt in this study, such as *cyc2* genes encoding membrane cytochrome *c*; *cyc1* genes encoding cytochrome *c*4; and *coxA*, *coxB*, and *coxC* encoding cytochrome *c* oxidases. The relative abundances of these predicted Fe(II) oxidation genes in treatments without As(III) was higher than that in treatments with As(III), indicating that As(III) might inhibit the Fe(II) oxidation process. These changes were in line with the observation that the rate of Fe(II) oxidation was higher in treatments without As(III) (Figure 1A). The ribulose-1,5-bisphosphate carboxylase/oxygenase (Rubisco) was the main pathway predicted to be involved in carbon fixation in all treatments, and had a greater predicted abundance in incubations without As. This was consistent with the greater carbon fixation in the absence of As(III) (Figure 3). The predicted genes related to As transportation and transformation were diverse, including *arsA* (encoding arsenical transporting ATPase), *ACR3* (encoding arsenite transporter), *arsH* (encoding As resistance protein), and *aioA* and *aioB* (encoding arsenite oxidase) and were predicted from all treatments. The analysis showed that *aioA* was predicted to be substantially more abundant than other As metabolism genes in all treatments. In addition, the relative abundance of predicted *aioA* in treatments with As(III) was much higher than that in treatments without As(III) (Figure S11). This prediction was consistent with the qPCR of *aioA* genes from different treatments (Figure 5). The

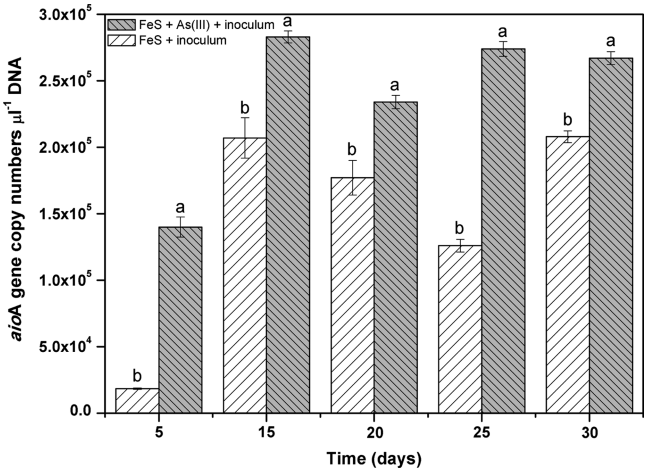

Figure 5. Copy numbers of the *aioA* gene in biogenic Fe(III) (oxyhydr)oxides in the absence or presence of As. Significant differences are indicated by different letters ($P < 0.05$). Error bars show the standard deviation of the three replicates.

qPCR results showed that incubations with As(III) resulted in two or three times higher abundances of *aioA* genes compared to incubations without As(III), indicating that As(III) could simulate the expression of As(III) oxidation genes.

DISCUSSION

Paddy soil ecosystems are sites of rapid biogeochemical cycling of iron and carbon because of periodic changes of the oxic soil surface and deeper anoxic soils.[33] Long-term waterlogging results in reducing the soil conditions, which causes Fe(II) accumulation by the activity of Fe(III)-reducing bacteria. Dissolving Fe(III) minerals promotes As release and mobility, posing a potential threat of secondary contamination of As. However, the reoxidation of Fe(II) by Fe(II)-oxidizing bacteria occurs at the same time because of the limited amount of dissolved oxygen.[12,13] Fe(II)-oxidizing bacteria are typically found growing at oxic−anoxic interfaces and are generally microaerophilic bacteria.[34] In karstic soils, the thin soil layer and the high hydraulic conductivity allow oxygen to easily diffuse into the soil to form an oxic−anoxic interface that promotes microaerophilic bacteria growth. In addition, available oxygen in the rhizosphere through the root aerenchyma could create a mosaic of aerobic microsites for microaerophilic Fe(II)-oxidizing bacteria growth, promoting Fe(II) oxidation around rhizosphere even in flooded conditions.[33] These new Fe(III) minerals formed in micro-oxic zones under flooded conditions could re-sequester As and prevent rice root uptake of As.[35] The abundance of these microaerophilic Fe(II)-oxidizing bacteria could be up to 1% of the total rhizosphere microbial population.[36] In these restricted niches that provide low concentration of oxygen, Fe(II)-oxidizing bacteria could actively compete with rapid abiotic process controlling Fe(II) oxidation.[11] Previous field work and laboratory measurements indicate that there is a significant microbial component to Fe(II) oxidation under such conditions, and the maximum biotic rate of Fe(II) oxidation could account for 88% of the total Fe(II) oxidation at oxygen levels below 50 μM.[12,13,37] Even when the oxygen concentration is low, a small amount of abiotic Fe(II) oxidation exists.[37]

In the present study, several microaerophilic bacteria were found in the growth bands formed in the gradient tube inoculated with iron-rich karstic paddy soil, including *Cupriavidus*, *Bradyrhizobium*, *Kaistobacter*, *Polaromonas* and *Pseudomonas*, and all incubations were consistent with micro-oxic Fe(II) oxidation as described in previous reports under similar conditions.[38−40] The difference of carbon fixation and As(III) oxidation in inoculated and controlled treatments supported that these processes were driven by microaerophilic bacteria. Many of the known bacteria involved in Fe(II) oxidation are chemolithoautotrophic that can conserve the energy for inorganic carbon fixation from the oxidation of reduced species, including Fe(II) and As(III).[7,41] During Fe(II) oxidation, various Fe(III) (oxyhydr)oxides produced by microaerophilic Fe(II)-oxidizing bacteria can coprecipitate and/or adsorb soluble As, which can significantly reduce the mobility and bioavailability of As.[21,42] Furthermore, the oxidation of As(III) to As(V) can increase As adsorption onto Fe(III) (oxyhydr)oxides and reduce the toxicity of As.[20]

Carbon Fixation during Microaerophilic Microbial Fe(II) Oxidation. In the present study, the incorporation of $^{13}C-NaHCO_3$ into the DNA demonstrated that bacteria within these communities are capable of carbon fixation under microaerophilic Fe(II)-oxidizing conditions. According to the percentage of ^{13}C-labeled biomass (Figure 3), the chemoautotrophic rate of carbon fixation in soils is estimated at 8.02 mmol C m^{-2} d^{-1},[43] which is comparable to carbon fixation rates in basaltic ocean by Fe(II) and sulfide oxidation.[44,45] Previous reports showed that the carbon fixation by chemolithoautotrophic bacteria was significant to the carbon cycle of the oceanic crust. In addition, the isotopic composition of total mat carbon implied that carbon dioxide fixation by Fe(II)-oxidizing bacteria could provide a source of organic carbon for heterotrophic bacteria.[10] Based on the above discussion, we hypothesized that

https://dx.doi.org/10.1021/acs.est.0c05791
Environ. Sci. Technol. 2021, 55, 3634−3644

carbon fixation coupled with Fe(II) oxidation could also be active and plays a role in the C−Fe cycle in karstic soils.

The bacteria responsible for carbon fixation were investigated by combining SIP with high-throughput sequencing approaches. Several community members in gradient tubes grew using ^{13}C−$NaHCO_3$ as a carbon source in the presence or absence of As (Figures 4 and S9 and S10). The microbial community in incubation with $NaHCO_3$ as the carbon source was markedly different from that of original inoculum (Figure S7). After incubation for 30 days, the results of PCoA analysis and α-diversity showed that the diversity of autotrophic microorganisms varied between treatments with and without As(III) (Figure S7 and Tables S5). The bacteria enriched in the As(III) treatment are likely able to tolerate As and overcome its toxicity.[20] Additionally, some autotrophic microorganisms can couple carbon fixation with As(III) oxidation,[27] which converts the more toxic species As(III) into the less toxic species As(V) (Figure S3), thus reducing As(III) uptake into the cell.[46]

The PICRUSt analysis-predicted carbon fixation metabolism genes belonging to most KEGG categories are shown in Figure S11. Genomic analyses have confirmed that the CBB pathway for carbon fixation, including Rubisco genes is present in isolated microaerophilic Fe(II)-oxidizing bacteria, such as *Mariprofundus ferrooxydans*, *Gallionella capsiferriformans*, and *Sideroxydans lithotrophicus*.[15] Deletion of the genes encoding Rubisco from Fe(II)-oxidizing bacteria led to a 96% reduction in $^{13}CO_2$ assimilation.[47] In this study, the Rubisco genes were predicted in all treatments, but there was no prediction of carbon fixation genes for other pathways, indicating that the main carbon fixation process might be through the CBB pathway.[15] In addition, the PICRUSt analysis showed that the presence of As suppressed the predicted abundance of organisms with a putative CBB pathway. This observation was corroborated by the decreased carbon fixation efficiency in the presence of As (Figure 3). However, the carbon assimilation data suggested that enriched microaerophilic bacteria are still able to express proteins for the CBB cycle in the presence of As.[27] The predicted Rubisco small and large subunit genes are associated with Rubisco form II, which was found in most microaerophilic Fe(II)-oxidizing bacteria genes.[15,17] Form II enzymes are adapted to low O_2 and high CO_2 conditions,[17] which is consistent with the microaerobic lifestyle. Therefore, the micro-oxic zones found in paddy soils and root nodules might be zones for carbon fixation via Form II enzymes by microaerophilic Fe(II)-oxidizing bacteria.

DNA-SIP combined with 16S rRNA gene amplicon sequencing was adopted to identify potential microorganisms related to carbon fixation. The genera *Cupriavidus* and *Kaistobacter* were significantly enriched in the 16S rRNA gene pool from the ^{13}C-enriched DNA fractions than in the ^{12}C DNA fractions and identified as likely autotrophs in treatments with or without As(III). Specially, *Cupriavidus* exhibited the highest relative abundance in ^{13}C-heavy fractions (>45%), suggesting its key role as a chemolithoautotroph in these soils. *Cupriavidus* have been extensively studied not only for their expression of CBB gene systems, which encoded the energy-demanding CBB reductive pentose−phosphate cycle,[48,49] but also in Fe(II) oxidation within micro-oxic environments.[38] In this study, the high relative abundance of the carbon-fixing microorganism and predicted functional genes of carbon fixation indicate that the microorganism might fix carbon via the CBB pathway. Previous studies have documented that *Kaistobacter* is able to oxidize Fe(II).[40] However, there are no reports showing *Kaistobacter* growing chemolithoautotrophically. The enrichment of *Kaistobacter* in ^{13}C-heavy fractions may result from the incorporation of the ^{13}C-carbon from the ^{13}C-labeled metabolites or dead biomass.

The other four genera enriched in ^{13}C-carbon treatments without As(III), that is, *Bradyrhizobium*, *Mesorhizobium*, *Hyphomicrobium*, and *Rhizobium*, belong to the family of *Rhizobiales*. The high abundance of these four genera in ^{13}C-heavy fractions (Figure S9) indicated that they participated in carbon assimilation in the gradient tubes. *Bradyrhizobium* furthermore has a demonstrated capacity for Fe(II) oxidation and carbon fixation.[38,50] *Mesorhizobium* and *Rhizobium* can produce and import siderophores[51] that are able to accelerate the solubilization of Fe(III) minerals, avoiding encrustation of the cell surface with the Fe(III) minerals they produce.[52] Furthermore, these two bacteria have the capacity to oxidize carbon monoxide through carbon monoxide dehydrogenase.[53] Members of *Hyphomicrobium* are able to use organic matter as a carbon source.[54] Their enrichment in the ^{13}C-heavy fractions suggested that *Hyphomicrobium* may use either inorganic or organic carbon sources for growth. In treatments with As(III), unclassified *Phycisphaerales* and *Opitutaceae* were enriched in the ^{13}C-heavy fractions. *Phycisphaerales* belong to *Planctomycetes* and may catalyze As(III) oxidation in mildly As-contaminated sediments[55] as well as utilize all sorts of carbon compounds.[56] Previously, *Opitutaceae* was observed in a microbial community involved in As oxidation in estuarine wetlands.[57] Although the roles of these two bacteria in carbon fixation in soil were not definitively determined in the present study, we obtained direct evidence of carbon fixation by these bacteria under Fe(II)- and As(III)-oxidizing conditions by combining DAN-SIP with high-throughput sequencing using labeled inorganic carbon compounds as the substrate.

As(III) Oxidation and Sequestration Coupled with Fe(II) Oxidation. Fe(III) (oxyhydr)oxides have large surface areas and a number of available surface binding sites, which control the amount of As that can be adsorbed.[22,58] Several studies have shown that poorly crystalline ferrihydrite has a higher density of sorption sites for As adsorption compared to more crystalline iron oxides.[20,25] During Fe(II) oxidation, the presence of inorganic ligands, such as SO_4^{2-}, PO_4^{3-}, and AsO_4^{3-}, can inhibit the development of Fe(III) (oxyhydr)oxide crystallinity.[59] These adsorbing ions on ferrihydrite produce minerals with smaller particle size and lower crystallinity[20,60] and prevent the transformation of ferrihydrite into more crystalline products. Besides these inorganic ligands, the carboxylic and dicarboxylic acids excreted by Fe(II)-oxidizing bacteria could cover the mineral surfaces,[23,52] which could decrease As adsorption by blocking the reactive sites. However, no significant concentrations of these organic acids were detected in culture medium (data not shown), suggesting that the effect of these free organic ligands on As adsorption could be negligible. In addition, the results showed that Fe(II)-oxidizing bacteria excrete extracellular polymeric substances (EPS) composed primarily of polysaccharides and proteins,[61] which can coat Fe(III) (oxyhydr)oxides to form cell−EPS−mineral aggregates (Figure S12). A previous report showed that the EPS and matrices of cell−EPS−mineral aggregates could provide significant sorption and binding sites for heavy metals.[60] The reactive groups in EPS could promote As sorption to Fe(III) (oxyhydr)oxide substrates in mineral bacteria suspensions.[62] Based on the above discussion and greater capacity of As sequestration in the inoculated treatments, it seems that the

https://dx.doi.org/10.1021/acs.est.0c05791
Environ. Sci. Technol. 2021, 55, 3634−3644

organics excreted by Fe(II)-oxidizing bacteria could enhance As immobilization in this study. However, extracellular carbon species could have an ambiguous impact on As sorption to Fe(III) (oxyhydr)oxide because of the different chemical characterizations among carbon species.[62−64] Further work to develop As-sensitive fluorescence labeling in combination probes for DNA or EPS by CLSM might determine the relationship between As sequestration and the cell−EPS−Fe(III) mineral aggregates.[65]

Our results showed that As(III) oxidation occurred under micro-oxic conditions. Over 80% As(III) was oxidized in the inoculated treatments, while only ∼6% of As(III) was oxidized in the abiotic incubations (Figure S3A). These results highlight the importance of the microbial As(III) oxidation to overall As sequestration. In addition, the detection of *aioA* genes as well as the prediction by PICRUSt suggest that microbially mediated As(III) oxidation occurred under microaerophilic Fe(II) oxidation (Figures 5 and S11). Microbial oxidation of As(III) to As(V), which is less toxic and less mobile than As(III), is a common microbial detoxification mechanism that is encoded for by the *aioA* gene (Figure 5).[33] In a previous study, the *aioA* gene was found to be almost ten times more abundant than other As metabolism genes in paddy soils, indicating a high potential for microbial As(III) oxidation.[66] *Cupriavidus*, *Pseudomonas*, *Polaromonas*, and *Ralstonia*, all enriched in As(III) incubations, have been reported to contain homologues of genes encoding *aioA*.[67,68] These bacteria are known to oxidize As(III) as well as Fe(II) under micro-oxic conditions.[39,42] Microorganisms encoding the *aioA* gene could have actively contributed to the high As(V) concentrations in Fe(III) (oxyhydr)oxides observed in previous studies.[21] Previous results also support that incorporation of As(V) to Fe(III) (oxyhydr)oxides formed by Fe(II)- or As(III)-oxidizing bacteria can reduce the dissolved As concentrations.[24]

Generally, Fe(III) (oxyhydr)oxides have a higher adsorption capacity for As(V) than As(III) when the pH is below 7.[36] The oxidation of As(III) to As(V) will promote As sequestration by Fe(III) (oxyhydr)oxides in the present study. During As oxidation and sequestration, As(III) was the dominant species in the culture medium while almost all As was As(V) in the co-precipitation (Figure S3), indicating that As(V) was preferentially partitioned into Fe(III) (oxyhydr)oxides. A previous report showed that the microaerophilic microorganisms were covered with Fe(III) (oxyhydr)oxides,[24] which might prevent direct As(III) oxidation in the medium. The adsorbed As extracted with NaOH showed that As(III) and As(V) could both adsorb on Fe(III) (oxyhydr)oxides and the fraction of As(V) increased over the incubation time (Figure S3B). After formation of Fe(III) (oxyhydr)oxides, these adsorbed As(III) increased the contact between the microorganisms and As and could lead to a strengthening in As(III) biological oxidation. Then, the form of As(V) co-precipitated with Fe(III) (oxyhydr)oxides, which is consistent with the previous reports that As(V) was the dominant species in biogenic Fe(III) (oxyhydr)oxides in As-contaminated environments.[46,69] These results also demonstrated that co-precipitation performed better in As(V) removal than As(III) removal (Figures S3B and S6), in line with the notion that As(V) was preferentially partitioned into the solid phase.[24,70] The higher co-precipitation of As(V) by Fe(III) (oxyhydr)oxides might be because of the maximization of the number of coordination sites that provide a better chance of interaction between As(V) and Fe(III).[71] The analysis of XRD and Mössbauer results from Figures S4 and S5 suggests that some As was co-precipitated into ferrihydrite to form poor crystalline ferric arsenate during microbial Fe(II) oxidation. These coincide with previous findings that As preferentially co-precipitated rather than adsorbed to Fe(III) minerals,[32,39] which could better stabilize As during subsequent recrystallization.[23]

The proposed mechanism for the As sequestration in contaminated paddy soils affected by rocky soil desertification is illustrated in Figure 6. The results demonstrated that the

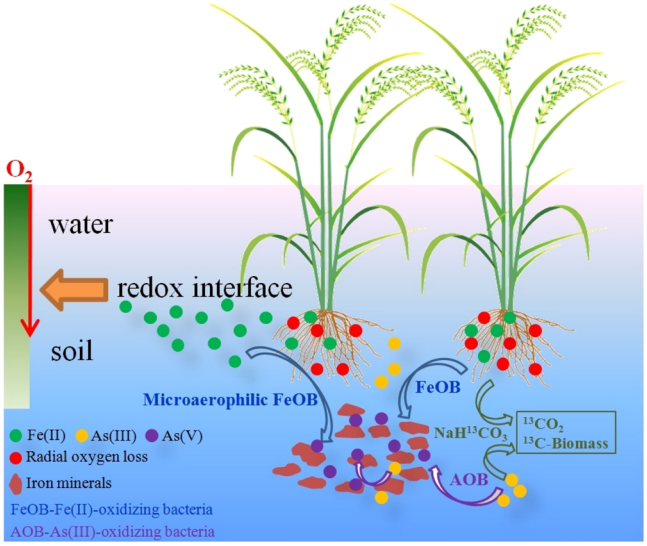

Figure 6. Schematic illustration of As(III) sequestration and carbon fixation by microaerophilic bacteria during microbial Fe(II) oxidation.

microbial community enriched from karstic paddy soil was able to assimilate carbon dioxide during micro-oxic Fe(II) and As(III) oxidation, which detoxified As. This suggests that the critical zone of inorganic carbon-enriched karstic soils could provide a niche in paddy field for Fe−C transformation by microaerophilic Fe(II)-oxidizing bacteria. In addition, the Fe(III) (oxyhydr)oxides formed by Fe(II)-oxidizing bacteria had high surface area and reactivity and were able to sequester As through adsorption, coprecipitation, and secondary mineral formation, reducing its dissolved concentrations. Furthermore, oxidation of As(III) into As(V) by Fe(II)- and As(III)-oxidizing bacteria could promote As adsorption on Fe(III) (oxyhydr)-oxides. This study provides further evidence that microaerophilic Fe(II)-oxidizing bacteria could be explored for diverse roles related to resilience and remediation of ecosystems affected by natural geogenic sources and anthropogenic activities.

■ ASSOCIATED CONTENT

Supporting Information

The Supporting Information is available free of charge at https://pubs.acs.org/doi/10.1021/acs.est.0c05791.

Images of Fe(III) (oxyhydr)oxide band morphology in semisolid gradient media after four transfers and compared to abiotic incubations, SO_4^{2-}concentration around growth bands in different treatments, concentrations of As(III) and As(V) in biogenic Fe(III) (oxyhydr)oxide in the presence of As(III) treatments with inoculums, fitted Mössbauer spectra of minerals formed by microaerophilic bacteria in the presence or

https://dx.doi.org/10.1021/acs.est.0c05791
Environ. Sci. Technol. 2021, 55, 3634−3644

absence of As(III) at 12 K after incubation for 30 days, X-ray diffractogram for the Fe(III) precipitates after incubation for 30 days in the absence or presence of As(III), arsenic recovery from Fe(III) (oxyhydr)oxide (sorption + co-precipitation) by NaOH and acid extraction, PCoA comparing the microbial composition in different treatments, qPCR for 16S rRNA distribution in all DNA fractions, microorganisms responsible for carbon fixation in incubations in the absence and presence of As, relative abundance of predicted genes related to carbon, iron, and As cycling within incubations, and CLSM images of cell−mineral aggregates of Fe(II)-oxidizing bacteria in the presence of As(III) (PDF)

AUTHOR INFORMATION

Corresponding Author

Chengshuai Liu − *State Key Laboratory of Environmental Geochemistry, Institute of Geochemistry, Chinese Academy of Sciences, Guiyang 550081, China; CAS Center for Excellence in Quaternary Science and Global Change, Xi'an 710061, China;* orcid.org/0000-0003-0133-0119; Email: liuchengshuai@vip.gyig.ac.cn

Authors

Hui Tong − *National-Regional Joint Engineering Research Center for Soil Pollution Control and Remediation in South China, Guangdong Key Laboratory of Integrated Agro-environmental Pollution Control and Management, Guangdong Institute of Eco-environmental Science & Technology, Guangdong Academy of Sciences, Guangzhou 510650, China; State Key Laboratory of Environmental Geochemistry, Institute of Geochemistry, Chinese Academy of Sciences, Guiyang 550081, China; Department of Geological and Atmospheric Sciences, Iowa State University, Ames 50011, Iowa, United States*

Chunju Zheng − *State Key Laboratory of Environmental Geochemistry, Institute of Geochemistry, Chinese Academy of Sciences, Guiyang 550081, China*

Bing Li − *Guangdong Provincial Engineering Research Center for Urban Water Recycling and Environmental Safety, Tsinghua Shenzhen International Graduate School, Tsinghua University, Shenzhen 518055, China;* orcid.org/0000-0002-7161-0477

Elizabeth D. Swanner − *Department of Geological and Atmospheric Sciences, Iowa State University, Ames 50011, Iowa, United States;* orcid.org/0000-0001-9507-0893

Manjia Chen − *National-Regional Joint Engineering Research Center for Soil Pollution Control and Remediation in South China, Guangdong Key Laboratory of Integrated Agro-environmental Pollution Control and Management, Guangdong Institute of Eco-environmental Science & Technology, Guangdong Academy of Sciences, Guangzhou 510650, China*

Yafei Xia − *State Key Laboratory of Environmental Geochemistry, Institute of Geochemistry, Chinese Academy of Sciences, Guiyang 550081, China*

Yuhui Liu − *State Key Laboratory of Environmental Geochemistry, Institute of Geochemistry, Chinese Academy of Sciences, Guiyang 550081, China*

Zengping Ning − *State Key Laboratory of Environmental Geochemistry, Institute of Geochemistry, Chinese Academy of Sciences, Guiyang 550081, China*

Fangbai Li − *National-Regional Joint Engineering Research Center for Soil Pollution Control and Remediation in South China, Guangdong Key Laboratory of Integrated Agro-environmental Pollution Control and Management, Guangdong Institute of Eco-environmental Science & Technology, Guangdong Academy of Sciences, Guangzhou 510650, China;* orcid.org/0000-0001-9027-9313

Xinbin Feng − *State Key Laboratory of Environmental Geochemistry, Institute of Geochemistry, Chinese Academy of Sciences, Guiyang 550081, China; CAS Center for Excellence in Quaternary Science and Global Change, Xi'an 710061, China;* orcid.org/0000-0002-7462-8998

Complete contact information is available at: https://pubs.acs.org/10.1021/acs.est.0c05791

Notes

The authors declare no competing financial interest.

ACKNOWLEDGMENTS

This research was supported by the National Science Foundation of China (41603127, 41921004, 41977291, and 41671240), the Frontier Science Research Programme of the CAS (QYZDB-SSW-DQC046), GDAS' Project of Science and Technology Development (2018GDASCX-0928 and 2019GDASYL-0301002), and the Science and Technology Foundation of Guangdong, China (2019A1515011482 and 2017BT01Z176).

REFERENCES

(1) Song, X.; Gao, Y.; Wen, X.; Guo, D.; Yu, G.; He, N.; Zhang, J. Carbon sequestration potential and its eco-service function in the karst area, China. *J. Geogr. Sci.* **2017**, *27*, 967−980.

(2) Huang, Q.; Cai, Y. Assessment of karst rocky desertification using the radial basis function network model and GIS technique: a case study of Guizhou province, China. *Environ. Geol.* **2006**, *49*, 1173−1179.

(3) Zhang, L.; Qin, X.; Tang, J.; Liu, W.; Yang, H. Review of arsenic geochemical characteristics and its significance on arsenic pollution studies in karst groundwater, Southwest China. *Appl. Geochem.* **2017**, *77*, 80−88.

(4) Zhou, Y.; Song, S.; Yang, Z.; Chen, B.; Zeng, F. Environmental geochemical response of soils along banks of a river to mines and mining activity in the upper reaches of the river: a case study of the diaojiang river drainage system, Guangxi, China. *Geol. Bull. China* **2005**, *24*, 71−77.

(5) Li, B.; Li, Z.; Sun, X.; Wang, Q.; Xiao, E.; Sun, W. DNA-SIP Reveals the diversity of chemolithoautotrophic bacteria inhabiting three different soil types in typical karst rocky desertification ecosystems in Southwest China. *Microb.Ecol.* **2018**, *76*, 976−990.

(6) Li, Q.; Wang, H.; Jin, Z.; Xiong, W.; Wu, X.; Zhang, Y.; Liu, C. The carbon isotope fractionation in the atmosphere−soil−spring system associated with CO_2-fixation bacteria at Yaji karst experimental site in Guilin, SW China. *Environ. Earth Sci.* **2015**, *74*, 5393−5401.

(7) Kelly, D. P.; Wood, A. P.*The Chemolithotrophic Prokaryotes.The Prokaryotes*; Springer, 2006; pp 441−456.

(8) Reinthaler, T.; van Aken, H. M.; Herndl, G. J. Major contribution of autotrophy to microbial carbon cycling in the deep North Atlantic's interior. *Deep Sea Res., Part II* **2010**, *57*, 1572−1580.

(9) Hügler, M.; Sievert, S. M. Beyond the calvin cycle: autotrophic carbon fixation in the ocean. *Annu. Rev. Mar. Sci.* **2011**, *3*, 261−289.

(10) Jennings, R. M.; Whitmore, L. M.; Moran, J. J.; Kreuzer, H. W.; Inskeep, W. P. Carbon dioxide fixation by *Metallosphaera yellowstonensis* and acidothermophilic iron-oxidizing microbial communities from Yellowstone National Park. *Appl. Environ. Microbiol.* **2014**, *80*, 2665−2671.

(11) Emerson, D.; Moyer, C. Isolation and characterization of novel iron-oxidizing bacteria that grow at circumneutral pH. *Appl. Environ. Microbiol.* **1997**, *63*, 4784−4792.
(12) Druschel, G. K.; Emerson, D.; Sutka, R.; Suchecki, P.; Luther, G. W., III Low-oxygen and chemical kinetic constraints on the geochemical niche of neutrophilic iron (II) oxidizing microorganisms. *Geochim.Cosmochim. Acta* **2008**, *72*, 3358−3370.
(13) Maisch, M.; Lueder, U.; Kappler, A.; Schmidt, C. Iron lung: how rice roots induce iron redox changes in the rhizosphere and create niches for microaerophilic Fe(II)-oxidizing bacteria. *Environ. Sci. Technol. Lett.* **2019**, *6*, 600−605.
(14) St Clair, B.; Pottenger, J.; Debes, R.; Hanselmann, K.; Shock, E. Distinguishing biotic and abiotic iron oxidation at low temperatures. *ACS Earth Space Chem.* **2019**, *3*, 905−921.
(15) Kato, S.; Ohkuma, M.; Powell, D. H.; Krepski, S. T.; Oshima, K.; Hattori, M.; Shapiro, N.; Woyke, T.; Chan, C. S. Comparative genomic insights into ecophysiology of neutrophilic, microaerophilic iron oxidizing bacteria. *Front. Microbiol.* **2015**, *6*, 1265.
(16) Li, X.; Mou, S.; Chen, Y.; Liu, T.; Dong, J.; Li, F. Microaerobic Fe(II) oxidation coupled to carbon assimilation processes driven by microbes from paddy soil. *Sci. China Earth Sci.* **2019**, *62*, 1719−1729.
(17) Badger, M. R.; Bek, E. J. Multiple Rubisco forms in proteobacteria: their functional significance in relation to CO_2 acquisition by the CBB cycle. *J. Exp. Bot.* **2008**, *59*, 1525−1541.
(18) Tong, H.; Liu, C.; Li, F.; Luo, C.; Chen, M.; Hu, M. The key microorganisms for anaerobic degradation of pentachlorophenol in paddy soil as revealed by stable isotope probing. *J. Hazard. Mater.* **2015**, *298*, 252−260.
(19) Tong, H.; Chen, M. J.; Li, F. B.; Liu, C. S.; Li, B.; Qiao, J. T. Effects of humic acid on pentachlorophenol biodegrading microorganisms elucidated by stable isotope probing and high-throughput sequencing approaches. *Eur. J. Soil Sci.* **2018**, *69*, 380−391.
(20) Hohmann, C.; Winkler, E.; Morin, G.; Kappler, A. Anaerobic Fe(II)-oxidizing bacteria show As resistance and immobilize As during Fe(III) mineral precipitation. *Environ. Sci. Technol.* **2009**, *44*, 94−101.
(21) Fernandez-Rojo, L.; Héry, M.; Le Pape, P.; Braungardt, C.; Desoeuvre, A.; Torres, E.; Tardy, V.; Resongles, E.; Laroche, E.; Delpoux, S.; Joulian, C.; Battaglia-Brunet, F.; Boisson, J.; Grapin, G.; Morin, G.; Casiot, C. Biological attenuation of arsenic and iron in a continuous flow bioreactor treating acid mine drainage (AMD). *Water Res.* **2017**, *123*, 594−606.
(22) Sowers, T. D.; Harrington, J. M.; Polizzotto, M. L.; Duckworth, O. W. Sorption of arsenic to biogenic iron (oxyhydr)oxides produced in circumneutral environments. *Geochim.Cosmochim. Acta* **2017**, *198*, 194−207.
(23) Mikutta, C.; Schröder, C.; Marc Michel, F. Total X-ray scattering, EXAFS, and Mossbauer spectroscopy analyses of amorphous ferric arsenate and amorphous ferric phosphate. *Geochim.Cosmochim. Acta* **2014**, *140*, 708−719.
(24) Tong, H.; Liu, C.; Hao, L.; Swanner, E. D.; Chen, M.; Li, F.; Xia, Y.; Liu, Y.; Liu, Y. Biological Fe(II) and As(III) oxidation immobilizes arsenic in micro-oxic environments. *Geochim.Cosmochim. Acta* **2019**, *265*, 96−108.
(25) Dixit, S.; Hering, J. G. Comparison of arsenic(V) and arsenic(III) sorption onto iron oxide minerals: implications for arsenic mobility. *Environ. Sci. Technol.* **2003**, *37*, 4182−4189.
(26) Sun, W.; Sierra-Alvarez, R.; Milner, L.; Oremland, R.; Field, J. A. Arsenite and ferrous iron oxidation linked to chemolithotrophic denitrification for the immobilization of arsenic in anoxic environments. *Environ. Sci. Technol.* **2009**, *43*, 6585−6591.
(27) Bryan, C. G.; Marchal, M.; Battaglia-Brunet, F.; Kugler, V.; Lemaitre-Guillier, C.; Lièvremont, D.; Bertin, P. N.; Arsène-Ploetze, F. Carbon and arsenic metabolism in Thiomonas strains: differences revealed diverse adaptation processes. *BMC Microbiol.* **2009**, *9*, 127.
(28) Chen, M.; Wang, D.; Zhang, B. Analysis of sudden incidents of secondary arsenic pollution. *Chin. Emerg. Manage* **2010**, *4*, 40−50.
(29) Liu, Z.; Lozupone, C.; Hamady, M.; Bushman, F. D.; Knight, R. Short pyrosequencing reads suffice for accurate microbial community analysis. *Nucleic Acids Res.* **2007**, *35*, No. e120.
(30) Chen, C.; Meile, C.; Wilmoth, J.; Barcellos, D.; Thompson, A. Influence of pO_2 on iron redox cycling and anaerobic organic carbon mineralization in a humid tropical forest soil. *Environ. Sci. Technol.* **2018**, *52*, 7709−7719.
(31) Van Herreweghe, S.; Swennen, R.; Vandecasteele, C.; Cappuyns, V. Solid phase speciation of arsenic by sequential extraction in standard reference materials and industrially contaminated soil samples. *Environ. Pollut.* **2003**, *122*, 323−342.
(32) Huhmann, B. L.; Neumann, A.; Boyanov, M. I.; Kemner, K. M.; Scherer, M. M. Emerging investigator series: As(V) in magnetite: incorporation and redistribution. *Environ. Sci.: Processes Impacts* **2017**, *19*, 1208−1219.
(33) Kumarathilaka, P.; Seneweera, S.; Meharg, A.; Bundschuh, J. Arsenic speciation dynamics in paddy rice soil-water environment: sources, physico-chemical, and biological factors-a review. *Water Res.* **2018**, *140*, 403−414.
(34) Roden, E. E. Microbial iron-redox cycling in subsurface environments. *Biochem. Soc. Trans.* **2012**, *40*, 1249−1256.
(35) Weiss, J. V.; Emerson, D.; Backer, S. M.; Megonigal, J. P. Enumeration of Fe(II)-oxidizing and Fe(III)-reducing bacteria in the root zone of wetland plants: implications for a rhizosphere iron cycle. *Biogeochemistry* **2003**, *64*, 77−96.
(36) Rentz, J. A.; Kraiya, C.; Luther, G. W.; Emerson, D. Control of ferrous iron oxidation within circumneutral microbial iron mats by cellular activity and autocatalysis. *Environ. Sci. Technol.* **2007**, *41*, 6084−6089.
(37) Shelobolina, E.; Konishi, H.; Xu, H.; Benzine, J.; Xiong, M. Y.; Wu, T.; Blöthe, M.; Roden, E. Isolation of phyllosilicate-iron redox cycling microorganisms from an illite-smectite rich hydromorphic soil. *Front. Microbiol.* **2012**, *3*, 134.
(38) Xiu, W.; Guo, H.; Liu, Q.; Liu, Z.; Zhang, B. Arsenic removal and transformation by *Pseudomonas* sp. strain GE-1-induced ferrihydrite: co-precipitation versus adsorption. *Water, Air, Soil Pollut.* **2015**, *226*, 167.
(39) Zou, Q.; An, W.; Wu, C.; Li, W.; Fu, A.; Xiao, R.; Chen, H.; Xue, S. Red mud-modified biochar reduces soil arsenic availability and changes bacterial composition. *Environ. Chem. Lett.* **2018**, *16*, 615−622.
(40) Jennings, R. d. M.; Moran, J. J.; Jay, Z. J.; Beam, J. P.; Whitmore, L. M.; Kozubal, M. A.; Kreuzer, H. W.; Inskeep, W. P. Integration of metagenomic and stable carbon isotope evidence reveals the extent and mechanisms of carbon dioxide fixation in high-temperature microbial communities. *Front. Microbiol.* **2017**, *8*, 88.
(41) Xiu, W.; Guo, H.; Shen, J.; Liu, S.; Ding, S.; Hou, W.; Ma, J.; Dong, H. Stimulation of Fe(II) oxidation, biogenic lepidocrocite formation, and arsenic immobilization by *Pseudogulbenkiania* sp. strain 2002. *Environ. Sci. Technol.* **2016**, *50*, 6449−6458.
(42) Boschker, H. T. S.; Vasquez-Cardenas, D.; Bolhuis, H.; Moerdijk-Poortvliet, T. W.; Moodley, L. Chemoautotrophic carbon fixation rates and active bacterial communities in intertidal marine sediments. *PLoS One* **2014**, *9*, No. e101443.
(43) Middelburg, J. J. Chemoautotrophy in the ocean. *Geophys. Res. Lett.* **2011**, *38*, L24604.
(44) Grosse, J.; van Breugel, P.; Boschker, H. T. S. Tracing carbon fixation in phytoplankton-compound specific and total ^{13}C incorporation rates. *Limnol.Oceanogr.: Methods* **2015**, *13*, 288−302.
(45) Oremland, R. S.; Stolz, J. F. Arsenic, microbes and contaminated aquifers. *Trends Microbiol.* **2005**, *13*, 45−49.
(46) Yu, J.; Dow, A.; Pingali, S. The energy efficiency of carbon dioxide fixation by a hydrogen-oxidizing bacterium. *Int. J. Hydrogen Energy* **2013**, *38*, 8683−8690.
(47) Przybylski, D.; Rohwerder, T.; Dilßner, C.; Maskow, T.; Harms, H.; Müller, R. H. Exploiting mixtures of H_2, CO_2, and O_2 for improved production of methacrylate precursor 2-hydroxyisobutyric acid by engineered *Cupriavidus necator* strains. *Appl. Environ. Microbiol.* **2015**, *99*, 2131−2145.
(48) Gao, R.; Liu, H.; Xun, L. Cytoplasmic localization of sulfide: quinone oxidoreductase and persulfide dioxygenase of *Cupriavidus pinatubonensis* JMP134. *Appl. Environ. Microbiol.* **2017**, *83*, No. e01820.

https://dx.doi.org/10.1021/acs.est.0c05791
Environ. Sci. Technol. 2021, 55, 3634−3644

(49) Li, H.; Li, J.; Lü, C.; Xia, Y.; Xin, Y.; Liu, H.; Xun, L.; Liu, H. FisR activates σ^{54}-dependent transcription of sulfide-oxidizing genes in *Cupriavidus pinatubonensis* JMP 134. *Mol. Microbiol.* **2017**, *105*, 373−384.
(50) Franck, W. L.; Chang, W.-S.; Qiu, J.; Sugawara, M.; Sadowsky, M. J.; Smith, S. A.; Stacey, G. Whole-genome transcriptional profiling of *Bradyrhizobium japonicum* during chemoautotrophic growth. *J. Bacteriol.* **2008**, *190*, 6697−6705.
(51) Arif, K.; Archana, G.; Desai, A. J. Engineering heterologous iron siderophore complex utilization in rhizobia: effect on growth of peanut and pigeon pea plants. *Appl. Soil Ecol.* **2012**, *53*, 65−73.
(52) Kappler, A.; Newman, D. K. Formation of Fe(III)-minerals by Fe(II)-oxidizing photoautotrophic bacteria. *Geochim.Cosmochim. Acta* **2004**, *68*, 1217−1226.
(53) King, G. M. Molecular and culture-based analyses of aerobic carbon monoxide oxidizer diversity. *Appl. Environ. Microbiol.* **2003**, *69*, 7257−7265.
(54) Aa, K.; Olsen, R. The use of various substrates and substrate concentrations by a *Hyphomicrobium* sp. isolated from soil: effect on growth rate and growth yield. *Microb.Ecol.* **1996**, *31*, 67−76.
(55) Halter, D.; Cordi, A.; Gribaldo, S.; Gallien, S.; Goulhen-Chollet, F.; Heinrich-Salmeron, A.; Carapito, C.; Pagnout, C.; Montaut, D.; Seby, F.; Van Dorsselaer, A.; Schaeffer, C.; Bertin, P. N.; Bauda, P.; Arsène-Ploetze, F. Taxonomic and functional prokaryote diversity in mildly arsenic-contaminated sediments. *Res. Microbiol.* **2011**, *162*, 877−887.
(56) Wiegand, S.; Jogler, M.; Jogler, C. On the maverick Planctomycetes. *FEMS Microbiol. Rev.* **2018**, *42*, 739−760.
(57) Zhang, S.Y.; Su, J.Q.; Sun, G.X.; Yang, Y.; Zhao, Y.; Ding, J.; Chen, Y.S.; Shen, Y.; Zhu, G.; Rensing, C.; Zhu, Y.G. Land scale biogeography of arsenic biotransformation genes in estuarine wetland. *Environ. Microbiol.* **2017**, *19*, 2468−2482.
(58) Wang, S.; Mulligan, C. N. Occurrence of arsenic contamination in Canada: sources, behavior and distribution. *Sci. Total Environ.* **2006**, *366*, 701−721.
(59) Toner, B. M.; Santelli, C. M.; Marcus, M. A.; Wirth, R.; Chan, C. S.; McCollom, T.; Bach, W.; Edwards, K. J. Biogenic iron oxyhydroxide formation at mid-ocean ridge hydrothermal vents: Juan de Fuca Ridge. *Geochim.Cosmochim. Acta* **2009**, *73*, 388−403.
(60) Cismasu, A. C.; Michel, F. M.; Tcaciuc, A. P.; Tyliszczak, T.; Brown, G. E., Jr. Composition and structural aspects of naturally occurring ferrihydrite. *C. R. Geosci.* **2011**, *343*, 210−218.
(61) Wingender, J.; Neu, T. R.; Flemming, H. C.*What are Bacterial Extracellular Polymeric Substances? Microbial Extracellular Polymeric Substances*: Springer, 1999; pp 1−19.
(62) Huang, J.H.; Elzinga, E. J.; Brechbuehl, Y.; Voegelin, A.; Kretzschmar, R. Impacts of *Shewanella putrefaciens* strain CN-32 cells and extracellular polymeric substances on the sorption of As(V) and As(III) on Fe(III)-(hydr) oxides. *Environ. Sci. Technol.* **2011**, *45*, 2804−2810.
(63) Hao, L.; Guo, Y.; Byrne, J. M.; Zeitvogel, F.; Schmid, G.; Ingino, P.; Li, J.; Neu, T. R.; Swanner, E. D.; Kappler, A.; Obst, M. Binding of heavy metal ions in aggregates of microbial cells, EPS and biogenic iron minerals measured in-situ using metal-and glycoconjugates-specific fluorophores. *Geochim.Cosmochim. Acta* **2016**, *180*, 66−96.
(64) Babechuk, M. G.; Weisener, C. G.; Fryer, B. J.; Paktunc, D.; Maunders, C. Microbial reduction of ferrous arsenate: biogeochemical implications for arsenic mobilization. *Appl. Geochem.* **2009**, *24*, 2332−2341.
(65) Okibe, N.; Koga, M.; Morishita, S.; Tanaka, M.; Heguri, S.; Asano, S.; Sasaki, K.; Hirajima, T. Microbial formation of crystalline scorodite for treatment of As(III)-bearing copper refinery process solution using *Acidianus brierleyi*. *Hydrometallurgy* **2014**, *143*, 34−41.
(66) Zhang, S.Y.; Zhao, F.J.; Sun, G.X.; Su, J.Q.; Yang, X.R.; Li, H.; Zhu, Y.G. Diversity and abundance of arsenic biotransformation genes in paddy soils from Southern China. *Environ. Sci. Technol.* **2015**, *49*, 4138−4146.
(67) Nitzsche, K. S.; Weigold, P.; Lösekann-Behrens, T.; Kappler, A.; Behrens, S. Microbial community composition of a household sand filter used for arsenic, iron, and manganese removal from groundwater in Vietnam. *Chemosphere* **2015**, *138*, 47−59.
(68) Paul, D.; Kazy, S. K.; Gupta, A. K.; Pal, T.; Sar, P. Diversity, metabolic properties and arsenic mobilization potential of indigenous bacteria in arsenic contaminated groundwater of West Bengal, India. *PLoS One* **2015**, *10*, No. e0118735.
(69) Keim, C. N. Arsenic in biogenic iron minerals from a contaminated environment. *Geomicrobiol. J.* **2011**, *28*, 242−251.
(70) Mitsunobu, S.; Hamanura, N.; Kataoka, T.; Shiraishi, F. Arsenic attenuation in geothermal streamwater coupled with biogenic arsenic-(III) oxidation. *Appl. Geochem.* **2013**, *35*, 154−160.
(71) Jia, Y.; Demopoulos, G. P. Adsorption of arsenate onto ferrihydrite from aqueous solution: influence of media (sulfate vs nitrate), added gypsum, and pH alteration. *Environ. Sci. Technol.* **2005**, *39*, 9523−9527.

https://dx.doi.org/10.1021/acs.est.0c05791
Environ. Sci. Technol. 2021, 55, 3634−3644